18

Stomatal Conductance Modeling to Estimate the Evapotranspiration of Natural and Agricultural Ecosystems

Giacomo Gerosa[1], Simone Mereu[2], Angelo Finco[3] and Riccardo Marzuoli[1,4]
[1]*Dipartimento Matematica e Fisica, Università Cattolica del Sacro Cuore, via Musei 41, Brescia*
[2]*Dipartimento di Economia e Sistemi Arborei, Università di Sassari,*
[3]*Ecometrics s.r.l., Environmental Monitoring and Assessment, via Musei 41, Brescia*
[4]*Fondazione Lombardia per l'Ambiente, Piazza Diaz 7, Milano*
Italy

1. Introduction

This chapter presents some of the available modelling techniques to predict stomatal conductance at leaf and canopy level, the key driver of the transpiration component in the evapotranspiration process of vegetated surfaces. The process-based models reported, are able to predict fast variations of stomatal conductance and the related transpiration and evapotranspiration rates, e.g. at hourly scale. This high–time resolution is essential for applications which couple the transpiration process with carbon assimilation or air pollutants uptake by plants.

2. Stomata as key drivers of plant's transpiration

Evapotranspiration from vegetated areas, as suggested by the name, has two different components: evaporation and transpiration. Evaporation refers to the exchange of water from the liquid to the gaseous phase over living and non-living surfaces of an ecosystem, while transpiration indicates the process of water vaporisation from leaf tissues, i.e. the mesophyll cells of leaves. Both processes are driven by the available energy and the drying potential of the surrounding air, but transpiration depends also on the capacity of plants to replenish the leaf tissues with water coming from the roots through their hydraulic conduction system, the xylem. This capacity depends directly on soil water availability (i.e. soil water potential), which contributes to the onset of the water potential gradient within the soil-plant-atmosphere continuum.
Moreover, since the cuticle -a waxy coating covering the leaf surface- is nearly impermeable to water, the main part of leaf transpiration (about 95%) results from the diffusion of water vapour through the stomata. Stomata are little pores in the leaf lamina which provide low-resistance pathways to the diffusional movement of gases (CO_2, H_2O, air pollutants) from

outside to inside the leaf and vice versa. Following complex signal pathways, environmental, osmotic and hormonal, stomata regulate their opening area and thus the water vapour loss from leaves. When the evaporative demand is bigger than the water replenishing capability from the xylem, stomata closes partially or even totally. High evaporative demands can be due to elevated air temperature, high leaf-to-air vapour pressure deficit (VPD), and intense winds. Stomatal closure can also be caused by high concentration of carbon dioxide in the mesophyll space.
Stomata, thus, directly control plant transpiration preventing plants from excessive drying, and acting as key drivers of water vapour movements from vegetated surfaces to the atmosphere.
This chapter illustrates the modelling techniques to predict the stomatal behaviour of vegetation at high-resolution time scale, and the related water fluxes.

3. Modelling stomatal behaviour: The Jarvis-Stewart model and the Ball-Berry model

Stomata play an essential role in the regulation of both water losses by transpiration and CO_2 uptake for photosynthesis and plant growth. Stomatal aperture is controlled by the turgor pressure difference between the guard cells surrounding the pore and the bulk leaf epidermis. In order to optimize CO_2 uptake and water losses in rapidly changing environmental conditions, plants have evolved the ability to control stomatal aperture in the order of seconds. Stomatal aperture responds to multiple environmental factors such as, solar radiation, temperature, drought, VPD, wind speed, and sub-stomatal CO_2 concentrations.
The availability of modern physiological instrumentation (diffusion porometers, gas-exchange analyzers) has allowed to measure leaf stomatal conductance (g_s) in field conditions and to study how environmental variables influence this parameter.
However, measurements of g_s by porometers and gas-exchange analyzers can be made only when foliage is dry, and long-term enclosure in measuring chamber may lead to changes in the physiological state of the leaves. Consequently measurements in the field are usually made intensively over selected periods of a few hours in selected days.
Furthermore, stomatal conductance values depend also upon the physiological condition of the plant, which relates to the weather of the previous days as well as to the previous season for perennial species.
Therefore it is important to have continuous g_s measurements over the whole vegetative season in order to improve the interpretation of other physiological data such as photosynthesis rate and carbon assimilation.
An alternative to very frequent measurements of g_s in the field is to predict them from models that describe its dependency on environmental factors. These models can be parameterized using the available field measurements conducted on occasional periods.
Furthermore, modeling appears the most effective tool for integration, simulation and prediction purposes concerning the effects of climatic global change on vegetation.
Stomatal conductance is among the processes that have been most extensively modeled during the last decades. In their excellent review, Damour et al. (2010) describe 35 stomatal conductance models classified as:

1. models based on climatic control only
2. models mainly based on the gs-photosynthesis relationship
3. models mainly based on an Abscisic Acid (ABA) control
4. models mainly based on the turgor regulation of guard cell.

The next paragraphs provides information on two early developed g_s models which are currently among the most widely used: the multiplicative model of Jarvis (1976) based on climatic control and later modified by Stewart (1988), and the Ball Berry model (1988), based on g_s-photosynthesis relationship.

3.1 The Jarvis-Stewart model

The stomatal conductance model developed by Jarvis (1976) can be defined as an empirical multiplicative model based on the observed responses of g_s to environmental factors. The assumption of this model is that the influence of each environmental factor on g_s is independent of the others and can be determined by boundary line analysis (Webb 1972).
The Jarvis model, in its first form, integrates the responses of g_s to light intensity, leaf temperature, vapour pressure deficit, ambient CO_2 concentration and leaf water potential, according to the following equation:

$$g_s = f(Q) \cdot f(T_l) \cdot f(VPD_l) \cdot f(C_a) \cdot f(\Psi) \quad (1)$$

where Q is the quantum flux density (μE $m^{-2}s^{-1}$), T_l is the leaf temperature (°C), VPD_l is the leaf-to-air vapour pressure deficit calculated at leaf temperature (kPa), C_a is the ambient CO_2 concentration (ppm) and Ψ is leaf water potential (MPa).
Stewart (1988) further implemented this model adopting the assumption that the functions of environmental variables have values between zero and unit and exert their influence reducing the maximum stomatal conductance of the plant (g_{smax}), a species-specific value depending on leaf stomatal density, that can be defined as the largest value of conductance observed in fully developed leaves – but not senescent – of well-watered plants under optimal climatic conditions (Körner et al., 1979). This value can be derived from field measurements conducted under the above mentioned optimal conditions.
Furthermore, in Stewart formulation, quantum flux density is replaced by global solar radiation, leaf temperature by air temperature, leaf-to-air vapour pressure deficit by air vapour pressure deficit and leaf water potential by soil moisture deficit measured in the first meter of soil (i.e. soil water content, SWC). Stewart also omitted $f(C_a)$ because the effect of CO_2 ambient concentrations was considered negligible: this simplification allows for an easier data collection to run the model, but it must be kept in mind that C_a change considerably among seasons and thus the simplification may lead to a considerable error, especially when the model is used for annual g_s behavior of evergreen species.
The model is defined by the following equation:

$$g_s = g_{smax} \cdot f(Q) \cdot f(T_a) \cdot f(VPD_a) \cdot f(SWC) \quad (2)$$

It is important to notice that f(Q) can also be replaced by the more specific f(PAR), based on the photosynthetically active radiation.
Each function has a characteristic shape described by the following equations:

$$f(Q) = 1 - exp^{-aQ} \quad (3)$$

$$f(T_a) = \frac{(T - T_{\min})}{(T_{opt} - T_{\min})} \left[\frac{(T_{\max} - T)}{(T_{\max} - T_{opt})} \right]^b \tag{4}$$

where $b = \frac{(T_{\max} - T_{opt})}{(T_{opt} - T_{\min})}$, $f(T_a) = 0.1$ when $T \leq T_{\min}$ or $T \geq T_{\max}$ and $f(T_a) = 1$ when $T = T_{opt}$

$$f(VPD) = \frac{(1 - 0.1) \cdot (c - VPD)}{(c - d)} \tag{5}$$

where $f(VPD) = 1$ when VPD $\leq d$ and $f(VPD) = 0.1$ when VPD $\geq c$

$$f(SWC) = 1 - exp\left[k(SWC - SWC_{\max})\right] \tag{6}$$

where $f(SWC) = 1$ when $SWC = SWC_{max}$

Since g_s depends on four major variables, field measurements do not usually show a clear relationship with any of the considered variables. Often, g_s is reduced below the value expected for a value of a single independent variable, as the result of the influences of the other variables. As a consequence, the coefficients of each function must be derived with boundary-line analysis, plotting all field measurements of relative g_s ($g_{srel} = g_s / g_{smax}$) against each environmental variable considered separately.

Provided that enough measurements have been adequately performed to cover variable space, the upper limit of the scatter diagram indicates the response of g_s to the particular independent variable, when the other variables are not limiting.

An example of boundary-line analysis is reported in figure taken from Gerosa et al. (2009):

The main criticism formulated against this kind of approach is that the interactive effects between environmental factors are not properly taken into account, since interactions are only partially explained by the multiplicative nature of the model which simply multiplies concomitant effects, avoiding any synergistic interaction.

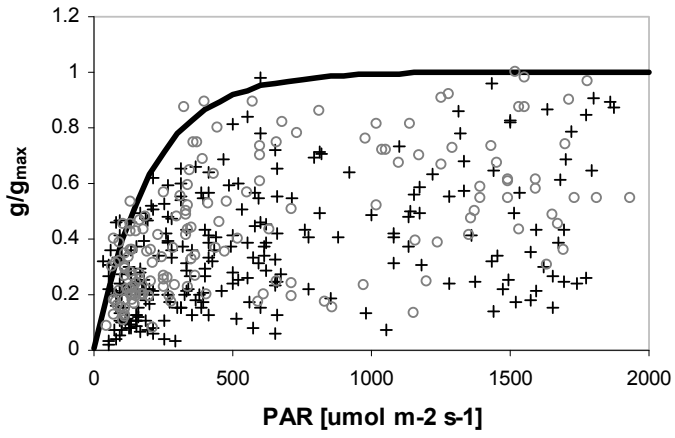

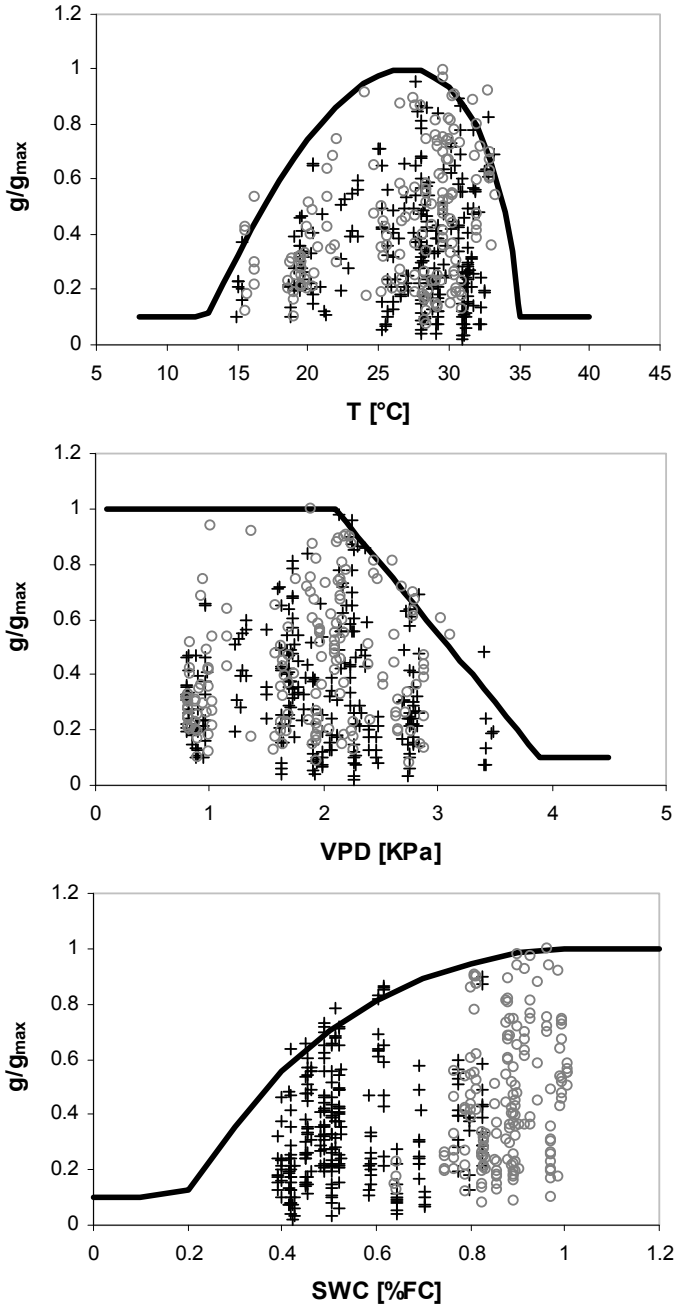

Fig. 1. Boundary-line analysis for the definition of g_s limiting function parameters (modified from Gerosa et al. 2008)

3.2 The Ball-Berry model

The Ball-Berry empirical model describes the behaviour of g_s as a function of environmental conditions and net photosynthetic rate. In its simplest form (Ball et al., 1987) the model states:

$$g_s = g_0 + a_1 An \frac{RH}{C_s} \tag{7}$$

Where g_s is the stomatal conductance to water vapour, g_0 is the stomatal conductance at the light compensation point, a_1 is a fitting parameter representing the slope of the equation, An is photosynthesis, RH is relative humidity and C_s is the molar fraction of CO_2 at the leaf surface. The model takes advantage of the feedback loop that exists between A and g_s (Farquhar at al., 1978) implying that they are interdependent. Additionally, An and g_s can respond independently to environmental variables and so they cannot be considered driving variables but rather state variables. The empirical relationship emerges from optimized vegetation behaviour that maximizes productivity (Patwardhan et al., 2006): the relationship, actually, corresponds roughly to the value of maximum surface conductance that maximizes productivity.

In order to derive g_s, the model needs to be coupled with a photosynthesis model (most often the Farquhar biochemical model) from which An is calculated. In order to derive g_s two equations must be solved simultaneously:

$$g_s = g_0 + a_1 An \frac{RH}{C_s} \tag{8}$$

$$A = (C_s - C_i) g_s \tag{9}$$

The problem is often solved by reiteration of the two equations where g_s at time t_{n+1} is computed with An at time t_n and An at time t_{n+2} is computed using g_s at time t+1. The reiteration approach however can give birth to oscillations in time of g_s and An due to chaotic solution in particular conditions. However, Baldocchi et al. (1994) found an analytical solution for the set of equations that bypasses this problem.

The original Ball-Berry model (Ball et al., 1987) was further implemented by Leuning (1995), considering that stomata respond to vapour pressure deficit (VPD) rather than humidity. In its modified version the equation takes the form:

$$g_s = g_0 + \frac{a_1 An}{(C_s - \Gamma)\left(1 + \frac{VPD_0}{VPD_s}\right)} \tag{10}$$

Where, Γ is the CO_2 compensation point, Cs and VPDs are the CO_2 concentration and vapour pressure deficit at the leaf surface, and VPD_0 is an empirical coefficient.

This model encapsulates two empirical trends reported in the literature. First, through the correlation between g_s and An the equation predicts that the ratio $(C_i\text{-}\Gamma)/(C_s\text{-}\Gamma)$ is largely independent of leaf irradiance and C_s, except near the light and CO_2 compensation points. It also predicts that g_s declines linearly as VPD_s increases, in fact through the relation

$$E = 1.6 \cdot g_s \cdot VPD_s \tag{11}$$

for the transpiration rate (E), the hyperbolic function of VPD_s is equivalent to a linear decline of g_s with increasing E.
The main limitation of the Ball-Berry-Leuning (BBL) model is its failure in describing stomatal closure in drought conditions. The model has been further implemented by Dewar (2002) to take SWC in consideration by coupling the BBL model with Tardieu model for stomatal response to drought. The coupled model takes the form:

$$g_s = \frac{a_1(An + Rd)}{Ci\left(1 + \frac{VPD_0}{VPDs}\right)} exp\left\{-\left[ABA\right]\beta exp(\delta\Psi)\right\} \quad (12)$$

Where Rd is dark respiration, $[ABA]$ is the concentration of abscisic acid in the leaf xylem, Ψ is the leaf water potential, β is the basal sensitivity of ion diffusion to $[ABA]$ at zero leaf water potential, and δ describes the increase in the sensitivity of ion diffusion to $[ABA]$ as Ψ declines.
The model has the advantage of describing stomatal responses to both atmospheric and soil variables and has proven to reproduce a number of common water use trends reported in the literature as, for example, isohydric and anisohydric behaviour.

4. Modelling water vapour exchange between leaves and atmosphere and scaling it up to plant and ecosystem level: The *big-leaf* approach and the resistive analogy

The exchange of water vapour through stomata is a molecular diffusion process since air in the sub-stomatal cavities is motionless as well as the air in the first layer outside the stomata directly in contact with the outer leaf surface, i.e. the leaf boundary-layer,. Outside the leaf boundary-layer, it is the turbulent movement of air that removes water vapour, and this process is two orders of magnitude more efficient than the molecular diffusion. The exchange of water between the plant and the atmosphere is further complicated by the physiological control that stomatal resistance exerts on the diffusion of water vapour to the atmosphere.
Transpiration is modelled through an electric analogy (Ohm's law) introduced by Chamberlain and Chadwick (1953). Transpiration behaves analogously to an electric current, which originates from an electric potential difference and flows through a conductor of a given resistance from the high to the low potential end (Figure 2).
The driving potential of the water flux E is assumed to be the difference between the water vapour pressure in ambient air $e(T_a)$ and the water vapour pressure inside the sub-stomatal cavity $e_s(T_l)$, the latter being considered at saturation. The resistances that water vapour encounters from within the leaf to the atmosphere is given by the resistance of the stomatal openings (r_s) and the resistance of the leaf boundary laminar sub-layer (r_b). This process can be represented by the following equation:

$$E = \frac{\left[e_s(T_l) - e(T_a)\right]}{r_b + r_s} \cdot \frac{\rho c_p}{\lambda\gamma} \quad (13)$$

where T_a is air temperature (°K), T_l is leaf temperature (°K), e is water vapour pressure in the ambient air (Pa), e_s is water vapour pressure of saturated air (Pa) and the term $\rho c_p/\lambda\gamma$ is a factor to express E in mass density units (kg m^{-2} s^{-1}), equivalent to mm of water per second,

being c_p the heat capacity of air at constant pressure (1005 J K^{-1} kg^{-1}), ρ the air density (kg m^{-3}), λ the vaporisation heat of water (2.5x10^6 J kg^{-1}), and $\gamma = c_p/\lambda$ the psychrometric constant (67 Pa K^{-1}). Despite the apparent difference with the well-known Penman-Monteith equation (Monteith, 1981), Eq. 13 is an equivalent formulation of this latter, as demonstrated by Gerosa et al. (2007).

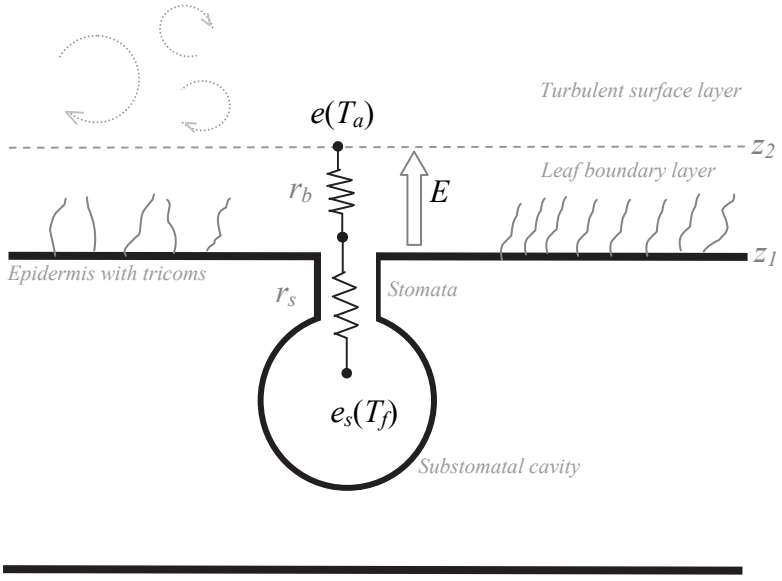

Fig. 2. Schematic picture of the transpirative process form a leaf. The symbols are explained in the text.

While the water vapour pressure deficit [$e_s(T_l)$-$e(T_a)$] driving the water exchange is determined by temperature difference, the amount of water flux is regulated by the resistances along the path of the flux.

The stomatal resistance r_s, reciprocal of the stomatal conductance g_s, is obtained applying one of the stomatal prediction models presented in the previous paragraph, which are fed by meteorological and agrometeorological data.

The quasi-laminar sub-layer resistance r_b depends on the molecular properties of the diffusive substance and on the thickness of the layer. The resistance against the diffusion of a gas through air is defined as:

$$r = \int_{z_1}^{z_2} \frac{1}{D_{H_2O}} dz \tag{14}$$

for the leaf boundary-layer the equation gives:

$$r_b = (z_2 - z_1)/D_{H2O} \tag{15}$$

where D_{H2O} is the diffusion coefficient of water vapour in the air, z_1 and z_2 representing the lower and upper height of the leaf boundary-layer.

However, the thickness of the leaf boundary-layer depends on leaf geometry, wind intensity and atmospheric turbulence. In order to take these factors in consideration, a more practical formulation, proposed by Unsworth et al. (1984), can be used:

$$r_b = k\left(d / u\right)^{1/2} \tag{16}$$

where k is an empirical coefficient set to a value of 132 (Thom 1975), d is the downwind leaf dimension, and u is the horizontal wind speed near the leaves.
The transpiration of a whole plant, or of a vegetated surface with closed canopy, may be modelled using a similar approach referred to as the *big-leaf*. The *big-leaf* assumes the canopy vegetation as an ideal big-leaf lying at a virtual height $z=d+z_0$ above ground (Figure 3). The d parameter is the displacement height, i.e. the height of the zero-plane of the canopy, equal to 2/3 of the canopy height, z_0 is the roughness length, i.e. the additional height above d where the wind extinguishes inside the canopy (sink for momentum), around 1/10 of the canopy height, and $d+z_0'$ is the apparent height of water vapour source.

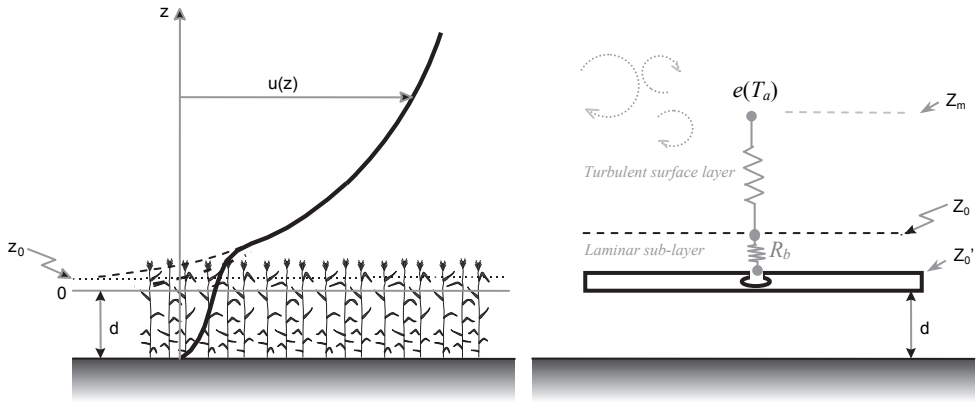

Fig. 3. The *big-leaf* approach to model water vapour exchange of a vegetated surface. Left side a real canopy; right side its big-leaf representation. The laminar sub-layer has been enlarged and the stomatal resistance is not shown. Please note the upper case notation of the resistances.

This transpiring big-leaf has a bulk stomatal resistance R_s equal to the sum of the stomatal resistances r_s of all the n leaves of the canopy. Recalling the rules of composition for parallel resistances:

$$1 / R_s = \sum_{1}^{n} 1 / r_s = n / r_s \tag{17}$$

Since the number of leaf is rarely known, a practical way of upscaling r_s is to consider the thickness of the "big-leaf" equal to the leaf area index of the canopy (LAI= $m^{-2}_{leaf}/m^{-2}_{ground}$)

i.e. the square meters of leaf area projected on each square meter of ground surface. This assumption is equivalent to stating that the light extinction coefficient of the big-leaf is equal to the light extinction of the canopy.
The transpiration rate of the "big-leaf", the whole canopy, is then obtained in a way very similar to those above developed for the leaves:

$$E = \frac{\left[e_s(T_l) - e(T_a)\right]}{R_a + R_b + R_s} \cdot \frac{\rho c_p}{\lambda\gamma} \tag{18}$$

It is worth noticing the upper case notation for the "bulk" resistances and the introduction of the aerodynamic resistance R_a.
The aerodynamic resistance depends on the turbulent features of the atmospheric surface layer, and it is introduced to account for the distance z_m at which the atmospheric water potential is measured above the canopy. It is formally the vertical integration of the reciprocals of the turbulent diffusion coefficients for all scalars, which in turn depends on the friction velocity u^* and the atmospheric stability. The integrated version of R_a is given by

$$R_a = \frac{1}{k \cdot u^*}\left[\ln\left(\frac{z_m - d}{z_0}\right) - \Psi_M\right] \tag{19}$$

where k is the von Kármán dimensionless constant (0.41), u^* is the friction velocity (m s^{-1}), a quantity indicating the turbulent characteristic of the atmosphere, and Ψ_M is the integrated form of the atmospheric stability function for momentum (non-dimensional).
The friction velocity, if not available, can be derived with the following equation:

$$u^* = \frac{k\, u_{zm}}{\ln\left(\frac{z_m - d}{z_0}\right) - \Psi_M} \tag{20}$$

where u_{zm} is the wind velocity measured at z_m, and Ψ_M is a function defined as:

$$\Psi_M = \begin{cases} 2\ln\left(\frac{1+y^2}{2}\right) \quad with \quad y = (1 - 16(z-d)/L)^{1/4} & if\ (z-d)/L < 0 \quad unstable\ condition \\ 0 & if\ (z-d)/L = 0 \quad neutral\ condition \\ -5(z-d)/L & if\ (z-d)/L > 0 \quad stable\ condition \end{cases} \tag{21}$$

L is the length (m) of Monin-Obukhov (1954) indicating the atmospheric stability:

$$L = \frac{-\rho\, c_p\, T_0\, u_*^{\,3}}{k\, g\, H} \tag{22}$$

with T_0 the reference temperature (273.16 K), g the gravity acceleration (9.81 m s^{-2}) and H the sensible heat flux (W m^{-2}).
Since L is a function of u^* and H, and vice versa, concurrent determination of u^* and Ψ_M from routine weather data would normally require an iterative procedure (Holtslag and van Ulden, 1983).

If the atmospheric stability is not known as well as the sensible heat flux, and the water potential in the atmosphere is measured near the canopy, a neutral stability can be assumed by setting Ψ_M=0 in the u^* equation with fairly good approximation.
The laminar sub-layer resistance R_b can by computed with a general purpose formulation proposed by Hicks et al. (1987) which involves the Schmidt and Prandtl numbers, being Sc=0.62 for water vapour and Pr=0.72 respectively:

$$R_b = \frac{2}{ku^*}\left(Sc / \Pr\right)^{2/3} \tag{23}$$

where k is here the von Kármán constant.
Modelling canopy transpiration using only three resistances in series might seem an oversemplification; however the approach has proven valid in different cases in predicting fast variations of water exchange over a vegetated surface following the stomatal behaviour, as well as to predict the total amount of transpired water (Grunhage et al., 2000).
To obtain a higher modelling performance, the resistive network of the "big-leaf" model can be implemented for specific needs. For example, multiple vegetation layers can be included in order to account for the transpiration of the understory vegetation below a forest, or the canopy can be decomposed in several layers, each with its own properties (De Pury and Farquhar, 1997) In such cases the models take the name of multi-layer models. Other improvements are required when multiple sources of water vapour have to be considered, for example when the evaporation from a water catchment, or evaporation from bare soil in ecosystems with sparse vegetation. .
All these models are collectively known as *1-D* SVAT models (one-dimensional Soil Vegetation Atmosphere Transfer models).
In the following paragraph a multi-layer dual-source model to predict the evapotranspiration from a poplar plantation ecosystem with understory vegetation is presented.

5. Example and applications - a multi-layer model for the transpiration of a mature poplar plantation ecosystem - comparison with eddy covariance measurements

The poplar plantation used for this modelling exercise was located in the Po valley near the city of Pavia. The ecosystem was made by mature poplar trees of about 27 m height with the soil below the plant mainly covered by poplar saplings and perennial grasses. Since the canopy was completely closed, most of the evapotranspiration was due to plants transpiration i.e. evaporation from other surfaces can be considered negligible. According to Choudhury and Monteith (1988), less than 5% of the water vapour flux is due to evaporation from soil for a closed canopy. In this case study evaporation from soil was strongly limited by the absence of tillage and by the coverage of understory vegetation. Moreover the upper soil layer resulted very dry and acted as a screen against water vapour transport from wetter underlying soil layers.
The water exchange was modelled using only two water sources, both of them transpirative: the poplar crown and the understory vegetation. Thus this example model includes only two layers (Figure 4).
The model is composed of three different sub-models: one stomatal sub-model for the stomatal conductance of the transpiring plants, one soil sub-model for the soil water content, and one atmospheric sub-model to describe the water vapour exchange dynamic at canopy level following the adopted resistive network.

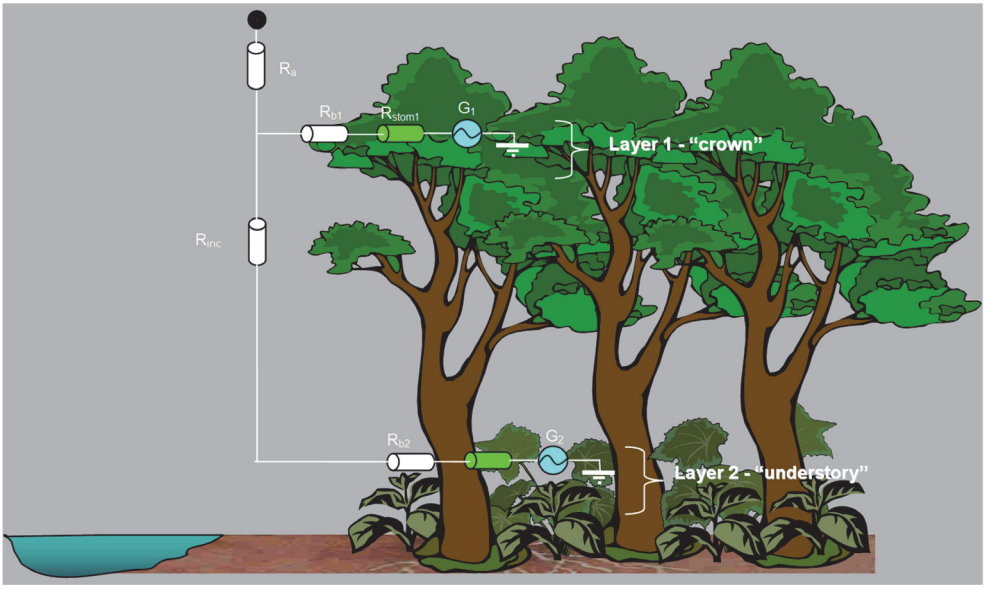

Fig. 4. A multi-layer multiple source model to estimate the water exchange between a poplar plantation ecosystem and the atmosphere.

5.1 The stomatal conductance sub-model

To describe the physiological behaviour of the bulk stomatal conductance (G_s) a Jarvis-Stewart multiplicative model was used, according to the following formulation:

$$G_s = g_{smax} \cdot [f(PHEN) \cdot f(T) \cdot f(PAR) \cdot f(VPD) \cdot f(SWC)] \quad (24)$$

where g_{smax} is the maximum stomatal conductance expressed by the poplar trees in non-limiting conditions. A maximum value of 1.87 cm s^{-1} (referred to the Projected Leaf Area) has been found in the literature for g_{smax} of poplar leaves located at 2 meter of height in Italian climatic condition (Marzuoli et al., 2009). This value has been reduced to 57% to account for the decreasing of g_{smax} with the canopy height, as proposed by Schafer et al. (2000). Thus a g_{smax} value of 0.8 cm s^{-1} was assumed for the canopy.

The phenology function *f(PHEN)* has been assumed equal to zero when the vegetation was without leaves and equal to one after the leaf burst when the leaves were fully expanded. This was fixed to the 110th day of the year (*DOY*).

Compared to Eq. 2, Eq. 24 includes a limiting function based on phenology *f*(*PHEN*) which grows linearly from 0 to 1 during the first 10 days after leaves emergence, and decreases linearly in the last 10 days, starting from *DOY* 285th, simulating leaf's senescence:

$$f(PHEN) = \begin{cases} 0 & \forall DOY \le SGS \quad or \quad \forall DOY \ge EGS \\ 1 & \forall (SGS + DayUp) < DOY < (EGS - DayDown) \\ ((\text{DOY - SGS}) \,/\, \text{DayUp}) & \forall\ SGS < \text{DOY} < (SGS + DayUp) \\ ((\text{EGS - DOY}) \,/\, \text{DayDown}) & \forall \quad (EGS - DayDown) < \text{DOY} < \text{EGS} \end{cases} \quad (25)$$

SGS and *EGS* are the days for the start and the end of the growing season respectively. . *DayUp* and *DayDown* are the number of days necessary to complete the new leaves expansion and to complete the leaves senescence, respectively.
The G_s dependence on light was modelled according to Eq. 3 form:

$$f(PAR) = 1 - exp^{-aPAR} \tag{26}$$

where *a* represents a specie-specific coefficient (0.006 in this study) and *PAR* is the Photosynthetically Active Radiation expressed as μmol photons m^{-2} s^{-1}.
Eq. 4 and Eq. 5 were used for *Gs* dependence on temperature and VPD, respectively.
For soil water content *SWC* a different limiting function, from that reported by Sterwart (1988), was used. The boundary-line analysis revealed that SWC exerted its influence on g_{smax} according to the following equation:

$$f(SWC) = \max\left\{0.1; \min\left[1; g \cdot SWC^{(h/SWC)}\right]\right\} \tag{27}$$

where *SWC* is expressed as fraction of soil field capacity while *g* and *h* are two coefficients whose values are respectively 1.0654 and 0.2951.
The bulk stomatal conductance of the understory vegetation was modelled using the same parameterization but assuming a g_{smax} value equal to 1.87 cm s^{-1}. The inherent approximation is that the understory vegetation was entirely composed of young poplar plantlets.

	Parameter	*Value*	*Unit*
	g_{max} (H_2O)	0.8	cm/s
f_{PHEN}	*SGS*	110	DOY
	EGS	285	DOY
	DayUp	10	Days
	DayDown	10	Days
f_{PAR}	*a*	0.006	adim.
f_T	T_{opt}	27	°C
	T_{max}	36	°C
	T_{min}	12	°C
	b	0.5625	adim.
f_{VPD}	*c*	3.7	KPa
	d	2.1	KPa
f_{SWC}	*g*	1.0654	adim.
	h	0.2951	adim.

Table 1. Values of the f limiting functions coefficients and g_{smax} for the stomatal conductance model of *Populus nigra*.

5.2 The soil sub-model

The water availability in the soil was modelled using a simple "bucket" model. In this paradigm the soil is considered as a bucket and the water content is assessed dynamically, step by step, via the hydrological balance between the water inputs (rains) and outputs (plant consumption) occurred in the previous time step. The model was initialised assuming the soil water saturated at the beginning of the season and assuming a root depth for soil exploitation of 3 m:

$$AWHC = (\theta_{FC}-\theta_{WP}) \cdot 1000 \cdot RootDepth = 243 \text{ mm } H_2O \text{ / } m^3 \text{ soil} \quad (28)$$

$$AW_t=0 = AWHC \text{ (mm)} \quad (29)$$

where $AWHC$ is the available water holding capability of the sandy soil between the wilting point (θ_{WP}= 0.114 m^3 m^{-3} for our sandy loam soil) and the field capacity (θ_{FC}=0.195 m^3 m^{-3}). The running equations were:

$$ET_{t-1} = F_{H20,\ t-1} \cdot 3600 \text{ / } \lambda \text{ (mm)} \quad (30)$$

$$AW_t = AW_{t-1} + Rain_{t-1} - ET_{t-1} \text{ (mm)} \quad (31)$$

$$SWC_t = AW_t \text{ / } AWHC \text{ (\% of FC)} \quad (32)$$

Eq. 32 represents the water loss of plant ecosystem through the transpiration of the two layers ($F_{H20,\ t-1}$) in the previous time step. Since water fluxes are expressed as rates (mm s^{-1}), for an hourly time step, as in our cases, their values must be multiplied by 3600 in order to get the water consumed in one hour.
AW_t is the available water in the soil after water inputs and consumptions. The effects of runoff and groundwater level rising have been neglected due to the flatness of the ecosystem and the groundwater level which were deeper than the root exploration depth.
SWC represents the soil water content expressed as percentage of field capacity, as requested by the $f(SWC)$ function of the stomatal sub-models.

5.3 The atmospheric sub-model and the resistive network

The resistance R_a was calculated by using Eq. 19 and Eq. 21, with z_m=33 m the measurement height, h= 26.3 m the canopy height, u^* the friction velocity, u the horizontal wind speed, L the Monin-Obhukhov length, d=2/3 $\cdot h$ the zero-plane displacement height and z_0=1/10 $\cdot h$ the roughness length.
The laminar sub-layer resistances of the layers 1 and 2 (R_{b1} and R_{b2}) were both calculated using the Eq. 23 given u^*.
The stomatal resistances of the layers 1 and 2 (R_{stom1} and R_{stom2}) were calculated using the stomatal sub-model after having estimated the leaf temperatures from the air temperature T and the heat fluxes H:

$$T_l = T + H \cdot (R_a + R_{b,\ heat}) \text{ / } (\rho \cdot c_p) \quad (33)$$

where $R_{b,heat}$ was calculated using the Eq. 23 with Sc=0.67 and Pr=0.71.
Then the vapour pressure deficit $VPD = e_s(T_l) - e(T)$ was derived from the T_l for the calculation of $e_s(T_l)$ and from the air temperature T and the relative humidity RH for the actual e: $e(T)=UR \cdot e_s(T)$.
The vapour pressure of the saturated air can be calculated from the well-known Teten-Murray empirical equation:

$$e_s(T) = 0.611 \cdot exp(17.269 \cdot (T - 273) \text{ / } (T - 36)) \quad (34)$$

which gives e_s in kPa when T is expressed as °K.
The stomatal resistance of the crown R_{stom1} was obtained as the reciprocal of the stomatal conductance obtained by the Jarvis–Stewart sub-model fed with PAR, T_{leaf}, VPD and SWC_t, the latter being the soil water content calculated with the Eq. 32 .

The understory R_{stom2} was obtained in a similar way but considering a understory g_{max} (=1.87 cm s^{-1}) and the *PAR fraction* reaching the below canopy vegetation instead of the original *PAR*:

$$PAR_{fraction} = \exp(-k \cdot LAI_1) \tag{35}$$

where k is the light extinction factor within the canopy, set to 0.54, and LAI_1 is the leaf area index of the crown, assumed to be equal to 2 at maximum leaf expansion.
The in-canopy resistance R_{inc} was calculated following Erisman et al. (1994):

$$R_{inc} = (14 \cdot LAI_1 \cdot h) / u^* \tag{36}$$

where h is the canopy height and LAI_1 the leaf area index of the crown.
The stomata of the big leaves of the two layers of Figure 4 (G_1 and G_2) were assumed as water generators driven by the difference of water concentration between the leaves (χ_{sat}), assumed water saturated al leaf temperature T_l, and the air (χ_{air}):

$$G_1 = G_2 = \chi_{sat} - \chi_{air} \quad (g\ m^{-3}) \tag{37}$$

where

$$\chi_{sat} = 2.165 \cdot e_s(T_l) / T_l \quad (g\ m^{-3})$$

$$\chi_{air} = 2.165 \cdot e(UR, T) / T \quad (g\ m^{-3})$$

being 2.165 the ratio between the molar weight of water molecules M_w (18 g mol^{-1}) and the gas constant R (8.314 J mol^{-1} K^{-1}) if e and e_s are expressed in Pa (multiplied by 1000 if expressed in kPa).
Then the total water flux of the ecosystem F_{H2O} could be calculated by composing all the resistances and the generators within the modelled resistive network, following the electrical composition rules for resistances and generators in series and in parallel, and applying the scaling strategy according to the *LAI*:

$$R_1 = (R_{b1} + R_{stom1} / LAI_1) \quad (s/m) \tag{38}$$

$$R_2 = (R_{b2} + R_{stom2} / LAI_2) \quad (s/m) \tag{39}$$

$$R_3 = R_{inc} + R_2 \quad (s/m) \tag{40}$$

$$G_{eq} = G_2 - (G_2 - G_1) \cdot R_3 / (R_1 + R_3) \quad (g\ m^{-3}) \tag{41}$$

$$R_{eq} = R_1 \cdot R_3 / (R_1 + R_3) \quad (s/m) \tag{42}$$

$$F_{H2O} = G_{eq} / (R_{eq} + R_a) / 1000 \quad (kg\ m^{-2}\ s^{-1} = mm\ s^{-1}) \tag{43}$$

where LAI_2 is the leaf area index of the understory vegetation (=0.5)

5.4 Comparison with EC measurements

Concurrent measurements of λE were performed over the same ecosystem by means of eddy covariance technique with instrumentation set-up according to Gerosa et al. (2005).

The comparison between the direct λE measurements and the modelled ones allowed the evaluation of model performance.
The model performance was very good in predicting the hourly variation of λE both during the summer season (*Modeled* = 0.885 · *Measured* + 8.4389; R^2=0.85, p<0.001, n=1872) with a slight tendency to underestimate the peaks.
An example of the comparison exercise for a summer week is shown in Figure 5

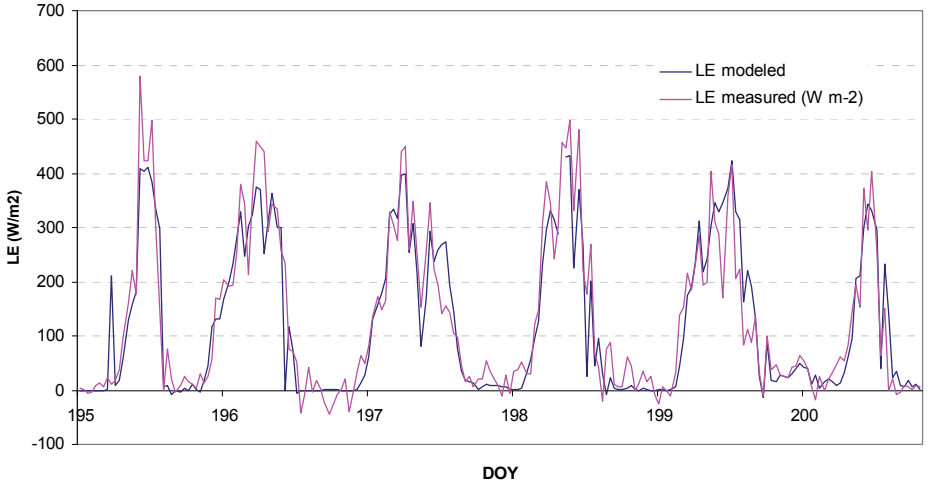

Fig. 5. Comparison between modelled and measured λE, expressed as W m^{-2} unit

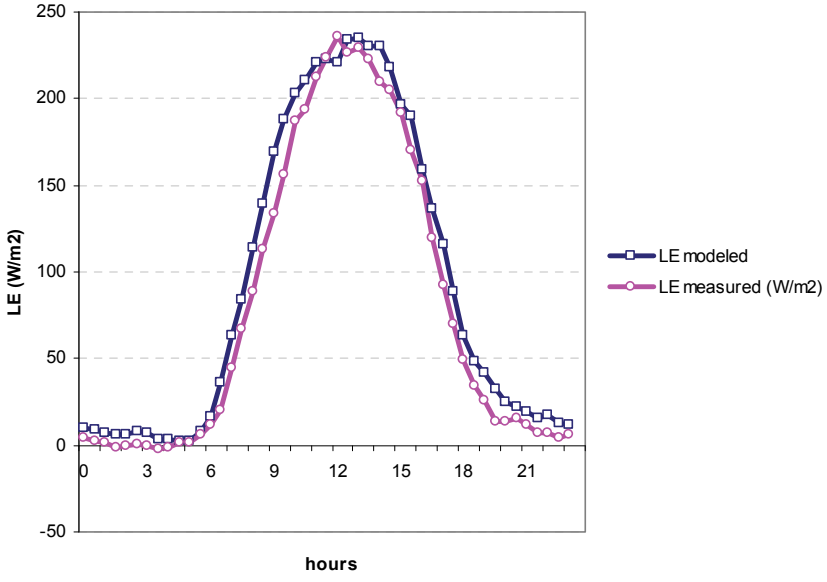

Fig. 6. Mean daily course of the modeled λE compared to the measured one. All the available hourly measurements were considered (n=3914)

For the whole year the performance was less good (*Modeled* = 0.876 · *Measured* + 21.443; R^2=0.68, p<0.001, n=3914) but still acceptable, especially in reproducing the average daily course of λE (Figure 6).

6. Conclusions

Scientific literature provides many ways (e.g. FAO) to estimate the evapotranspiration of a vegetated surface. Sometimes there is the need to predict this process at a very high-time resolution (e.g. hourly means). Hourly estimations of evapotranspiration, for example, are important in all the applications and the methodologies which couple transpiration process with carbon assimilation or air pollutants uptake by plants.
In these cases, the *big-leaf* approach, together with the resistive analogy which simulates the gas-exchange between vegetation and atmosphere, is a simple but valid example of a process-based model which includes the stomatal conductance behaviour, as well as a basic representation of the canopy features.

7. Acknowledgements

This publication was partially funded by the Catholic University's program for promotion and divulgation of scientific research.

8. References

Ball J.T., Woodrow I.E., Berry J.A., 1987. A model predicting stomatal conductance and its contribution to the control of photosynthesis under different environmental conditions. In: Biggins J, ed. *Progress in photosynthesis research*. Dordrecht: Martinus Nijhoff Publishers, 221-224

Chamberlain A.C., Chadwick R.C., 1953. Deposition of airborne radioiodine vapour. *Nucleonics* 11, 22–25

Choudhury B.J., Monteith J.L., 1988. A four-layer model for heat budget of homogeneous land surfaces. *Quarterly Journal of the Royal Meteorological Society* 114, 373–398

Damour G., Simonneau T., Cochard H., Urban L., 2010. An overview of models of stomatal conductance at leaf level. *Plant, Cell & Environment* 33, 1419-1438.

De Pury D.D.G., Farquhar G.D., 1997. Simple scaling of photosynthesis from leaves to canopies without the errors of big-leaf models. *Plant, Cell & Environment* 20, 537-557.

Dewar R.C., 2002. The Ball-Berry-Leuning and Tardieu-Davies stomatal models: synthesis and extension within a spatially aggregated picture of guard cell function. *Plant, Cell & Environment* 25: 1383-1398

Erisman J.W., Van Pul A., Wyers P., 1994. Parameterization of surface-resistance for the quantification of atmospheric deposition of acidifying pollutants and ozone. *Atmospheric Environment* 28, 2595–2607

Farquhar G.D., Dubbe D.R., Raschke K., 1978. Gain of the feedback loop involving carbon dioxide and stomata: theory and measurement. *Plant physiology* 62: 406-412

Gerosa G., Derghi F., Cieslik S., 2007. Comparison of Different Algorithms for Stomatal Ozone Flux Determination from Micrometeorological Measurements. *Water Air & Soil Pollution* 179, 309-321.

Gerosa G., Marzuoli R., Desotgiu R., Bussotti F., Ballarin-Denti A., 2008. Visible leaf injury in young trees of *Fagus sylvatica* L. and *Quercus robur* L. in relation to ozone uptake

and ozone exposure. An Open-Top Chambers experiment in South Alpine environmental conditions. *Environmental Pollution* 152, 274–284.

Gerosa G., Vitale M., Finco A., Manes F., Ballarin Denti A. and Cieslik S., 2005. Ozone uptake by an evergreen Mediterranean forest (*Quercus ilex*) in Italy. Part I: Micrometeorological flux measurements and flux partitioning. *Atmospheric Environment* 39, 3255-3266.

Grünhage L., Haenel H.D., Jager H.J., 2000. The exchange of ozone between vegetation and atmosphere: micrometeorological measurement techniques and models. *Environmental Pollution* 109, 373–392.

Hicks B.B., Baldocchi, D.D., Meyers T.P., Hosker R.P., Matt D.R., 1987. A Preliminary multiple resistance routine for deriving dry deposition velocities from measured quantities. *Water, Air and Soil Pollution* 36, 311–330.

Holtslag A.A.M., van Ulden A.P., 1983. A simple scheme for daytime estimates of the surface fluxes from routine weather data. *Journal of Climate and Applied Meteorology* 22, 517–529.

Jarvis P.G., 1976. The interpretation of the variations in leaf water potential and stomatal conductance found in canopies in the field. *Philosophical Transactions of the Royal Society of London*, Series B 273, 593–610.

Körner C., Scheel J., Bauer H., 1979. Maximum leaf diffusive conductance in vascular plants. Photosynthetica 13, 45-82.

Leuning R., 1995. A critical appraisal of a combined stomatal photosynthesis model for C3 plants. *Plant, Cell & Environment*. 18, 339–355.

Marzuoli R., Gerosa G., Desotgiu R., Bussotti F., Ballarin-Denti A., 2008. Ozone fluxes and foliar injury development in the ozone-sensitive poplar clone Oxford *(Populus maximowiczii x Populus berolinensis*): a dose–response analysis. Tree Physiology 29, 67-76.

Monin A.S., Obukhov A.M., 1954. Basic laws of turbulent mixing in the atmosphere near the ground. *Translation in Aerophysics of Air Pollution* (In: Fay, J.A., Hoult D.P. (Eds.), AIAA, New York, 1969, pp. 90–119). Akademija Nauk CCCP, Leningrad, TrudyGeofizich eskowo Instituta 151(24), 163–187.

Monteith J.L., 1981. Evaporation and surface temperature. *Quarterly Journal of the Royal Meteorological Society* 107, 1–27.

Patwardhan S., Pavlick, R. Kleidon A., 2006. Does the empirical Ball-Berry law of stomatal conductance emerge from maximization of productivity? *American Geophysical Union*, Fall Meeting 2006, abstract #H51C-0498.

Schafer K.V.R., Oren R., Tenhunen J.D., 2000. The effect of tree height on crown level stomatal conductance. *Plant, Cell & Environment* 23, 4 365-375.

Stewart J.B. (1988) Modelling surface conductance of pine forest. *Agricultural and Forest Meteorology* 43, 19–35.

Thom A.S., 1975. Momentum, mass and heat exchange of plant communities. In Vegetation and Atmosphere. Ed. J.L. Monteith. Academic Press, London.

Unsworth M.H., Heagle A.S., Heck W.W., 1984. Gas Exchange in open field chambers – I. Measurement and analysis of atmospheric resistance to gas exchange. Atmospheric *Environment* 18, 373–380.

Webb R.A., 1972. Use of the boundary line in the analysis of biological data. *Journal of Horticultural Science* 47, 309-319.